Neglected adsorbate interactions behind diffusion prefactor anomalies on metals

S. Ovesson,[1] A. Bogicevic,[2] G. Wahnström,[1] and B. I. Lundqvist,[1]
[1]*Department of Applied Physics, Chalmers University of Technology and Göteborg University, S-412 96 Göteborg, Sweden*
[2]*Scientific Research Laboratories, Ford Motor Company, Dearborn, Michigan 48121-2053*
(Received 20 February 2001; revised manuscript received 18 May 2001; published 11 September 2001)

Highly anomalous values for the preexponential factor in atomic diffusion rates at surfaces have recently been inferred from scanning-tunneling microscopy growth experiments. In an extensive first-principles kinetic Monte Carlo study, we show how long-range adsorbate interactions invalidate the standard nucleation-theory approach to analyzing experimental island-density data. When adatom-adatom interactions are properly accounted for in the analysis of experimental data, the anomaly is lifted, and deduced prefactors are consistent with direct theoretical calculations. We show that the dependence of the island density on the growth rate is modified by interactions, which could be used to identify adsorbate interactions in growth experiments.

DOI: 10.1103/PhysRevB.64.125423 PACS number(s): 68.43.Bc, 68.43.De, 68.43.Hn, 68.43.Jk

I. INTRODUCTION

The concept of thermally activated processes represents a cornerstone of modern materials physics. Almost all attempts at understanding the kinetics of chemical reactions, diffusion, and growth from an atomistic viewpoint assume—explicitly or implicitly—reaction rates that are vanishingly small at low temperatures, and increase exponentially with temperature. Quantitatively, the rate for a thermally activated process is given by transition-state theory[1–3] (TST) in the form of the celebrated Arrhenius law:

$$\nu = \nu_0 e^{-E_d/k_B T}, \tag{1}$$

where E_d is the activation energy, k_B the Boltzmann constant, and ν_0 the prefactor, which can be thought of as (but not identified with, see below) a vibration frequency characteristic of the system. Once the two parameters E_d and ν_0 have been deduced for all relevant elementary processes, the time evolution of a system can be predicted within the broad validity regime of TST.

Of the two parameters determining the rate of a process within TST, E_d and ν_0, the activation energy is unquestionably the more important one because it enters Eq. (1) exponentially. Less attention is generally paid to the prefactor, primarily because it enters the same equation only linearly. The justification for this uneven balance of attention comes from a vast amount of accumulated data for a wide variety of materials systems, which indisputably show that prefactors in single reaction steps, with few exceptions, assume a universal value of $\nu_0^* \sim 10^{13\pm1}\ \mathrm{s}^{-1}$.[4,5]

In the past few years, however, highly anomalous diffusion prefactors have been reported in experimental scanning-tunneling microscopy (STM) studies. Since STM is one of the primary atomic-resolution probes in modern surface science, and these deviations from standard values are of such enormous (up to ten orders of magnitude!) proportions, a rationalization of these observations is of critical importance. If exceedingly low prefactors are indeed a rare physical manifestation of certain materials systems, it remains to establish the origin of this anomaly, and explain why it is completely missed by state-of-the-art theoretical calculations (which by the way always fairly well reproduce experimentally measured activation energies).

Quite recently, Barth and coworkers[7] reported a remarkable trend in a compilation of experimental diffusion studies: whereas in systems with diffusion barriers in excess of 0.1 eV the prefactor is always near the expected value, i.e., $\nu_0 \simeq \nu_0^*$, it declines drastically as the activation energy drops below that limit ($\nu_0 \ll \nu_0^*$). This trend is based on STM growth studies,[7–9] but anomalously low prefactor values have been deduced also with other techniques.[10–14] No such trend is observed theoretically, where prefactors always come out ''normal,'' in stark disagreement with the experimental conclusions. As a radical reconciliation of this severe discrepancy, it has been suggested[7] that the harmonic approximation of TST, a pillar of modern rate theory, is invalid for diffusion processes on weakly corrugated surfaces.

In two recent papers,[15,16] theoretical state-of-the-art techniques have been used to critically evaluate the origin of anomalous diffusion prefactors. Both studies independently conclude that it is the customary way of interpreting experimental data rather than TST itself that fails for weakly corrugated systems: In Refs. 15 and 16, density-functional calculations for a total of three different metal-on-metal systems reveal long-range adsorbate interactions that, when accounted for in kinetic simulations, considerably distort the nucleation process. These indirect adatom-adatom interactions form a repulsive barrier to cluster nucleation, which results in an appreciable augmentation of the island density. When this surface morphology is interpreted in terms of a mean-field approach,[17] artificially low prefactors are incorrectly deduced. This conclusion is supported by the fact that in basically every instance where anomalous prefactors have been reported, the deduction process has relied on use of a mean-field approach neglecting adsorbate interactions.[18]

In a very recent publication, Michely *et al.* have argued that the Al/Al(111) growth experiment reported in Ref. 7 may have been distorted by contaminants.[19] By reducing the pressure of contaminants, this team was able to lift a large portion of the discrepancy between the data of Ref. 7 and mean-field theoretical predictions with normal prefactors, al-

though their results still show a lack of reproducibility. While at present it is unclear how reliable any island-density data for Al/Al(111) really are and whether contaminants could have been present in the other systems considered as well, there is still great incentive to study the effect of first-principles-calculated adsorbate interactions on the island density under perfect growth conditions.

In this study, we critically assess experimental and theoretical methods, including transition-state theory itself, in order to determine the likelihood of different explanations for the experimentally deduced anomalies in diffusion prefactors.

The paper is organized as follows: Section II contains a theoretical description of transition-state theory and its connections to diffusion prefactors, as well as a brief summary of the nucleation-curve approach for determining atomic diffusivities. Section III describes extensive first-principles calculations of adatom-adatom interaction energetics for three metal systems—Al/Al(111), Cu/Cu(111), and Al/Al(100)—and includes comparisons with existing models for adsorbate interactions. Kinetic simulations and results for the growth of Al(111) are presented and discussed in Sec. IV, while Sec. V contains our main conclusions. In the appendix, we present density-functional theory (DFT) calculations for the diffusion of Al on Au(111) and compare these results with experimental data.

II. SURFACE DIFFUSION

To get an idea of how experimental values for adsorbate diffusivities can disagree so patently with theoretical results in certain systems with exceedingly low activation energies, we first identify several error sources—experimental as well as theoretical ones. In the remainder of this section, we describe these deficiencies, and single out the most likely explanations for the observed discrepancies.

A. Diffusion theory

Thermally activated diffusion is quantitatively described by TST.[1] Assuming a classical, harmonic solid, the reaction rate is given by Vineyard's product formula:[20]

$$\nu = \frac{\prod_{i=1}^{3N} \nu_i^I}{\prod_{i=1}^{3N-1} \nu_i^T} \exp(-E_d/k_B T), \tag{2}$$

where ν_i^I and ν_i^T are the harmonic-vibration frequencies in the initial and transition states, respectively, and N denotes the number of particles in the system.[21] The diffusion prefactor ν_0, then, can be identified as the fraction in Eq. (2), and is a measure of the entropy at the transition state, as compared to that of the initial state. Usually these frequencies lie in the range 1–10 Thz, and the prefactor is therefore expected to lie in that range, as well. As an alternative to Eq. (2), the prefactor can be expressed in terms of integrals over the local phonon density of states in the equilibrium and transition states, respectively, as outlined in Ref. 22.

Our first concern is whether it is reasonable to expect very large prefactor deviations in thermally activated rate processes. In one sense, variations in the activation energy are actually coupled to variations in the prefactor. The frequencies ν_i^I that are most strongly coupled to the motion of the adatom are roughly proportional to the harmonic-vibration frequency of the potential-energy minimum at the binding site, which should scale linearly with $E_d^{1/2}$. The same can be said of the frequencies ν_i^T, but there will always be one more such frequency in the binding site entering Eq. (2). Hence, in general, a small activation energy is expected to be accompanied with a diminished prefactor via this so-called *compensation effect*.[23] However, this is a quite weak effect,[24,26] not nearly strong enough to explain reported anomalies in ν_0. In addition, it is hard to conjecture that several of the vibration frequencies entering in Eq. (2) should somehow conspire to raise or lower the prefactor so drastically, simply because the system dependence of ν_0 is suppressed by the cancellation of the ν_i^I's by the ν_i^T's. Indeed, if the substrate is not strongly perturbed by the motion of the adatom, the dependence of ν_0 on all frequencies other than those associated with the adatom may be neglected, as corroborated by semiempirical[25] and DFT-based[26] evaluations of the prefactor from Eq. (2). This amounts to the approximation that $N=1$ in Eq. (2).

If the motion of the adatom does perturb the substrate considerably, as in concerted motion or exchange with substrate atoms, the prefactor may differ from the universal value by one or two orders of magnitude. In all such cases, ν_0 is *increased* due to a relatively flat potential-energy landscape—i.e., involving much entropy—at the transition state.[27] A similar degeneracy at the binding site, required to explain a very small prefactor, is hard to imagine, and has never been demonstrated. For the same reason, anharmonic effects are expected to increase the prefactor in some cases, but never to decrease it.

Then the possibility remains that TST itself breaks down under certain circumstances. TST assumes that thermal equilibrium is established in binding sites between successive jumps, which excludes time correlation effects like long jumps[28,29] and multiple crossings of the saddle point between equilibrations. The validity of TST has been rigorously tested in molecular-dynamics simulations,[30,24] and the TST rate turns out to reproduce the dynamically measured (actual) rate very well even up to temperatures where $T \approx E_d/k_B$. However, those studies have not considered systems with very small activation energies ($\leqslant 0.1$ eV),[31] where anomalous diffusion behavior has been suggested to occur.[7]

In the early 1940s, Kramers showed that the TST rate represents an upper bound to the true escape rate, and that TST is valid for friction coefficients η of intermediate strength:[32]

$$\frac{\nu^I k_B T}{E_d} \leqslant \eta \leqslant 2\pi\nu^T. \tag{3}$$

(The parameters ν^I and ν^T represent the geometric means of the ν^I's and ν^T's, respectively.) For the low- and high-friction limits he deduced

$$\nu_0 = \eta E_d/(k_B T) \tag{4}$$

and

$$\nu_0 = 2\pi \nu^I \nu^T/\eta, \tag{5}$$

respectively.

The boundaries of the intermediate-friction regime can be estimated as follows: if friction is assumed to be dominated by phonons, η can be evaluated within the Debye model (see Ref. 4 and references therein):

$$\eta = \frac{3\pi^2 m(\nu^I)^4}{M\nu_D^3}, \tag{6}$$

where ν_D denotes the Debye frequency, and m and M are the masses of the adsorbed particle and the lattice atoms, respectively. For Al/Al(111) and Al/Au(111), for which extremely small prefactors have been reported, $\eta = 5\times 10^{13}$ s^{-1} and 5×10^{14} s^{-1}, respectively. With these estimates, thus, both systems are in the high-friction regime, but applying Eq. (5) changes ν_0 by less than an order of magnitude from the TST value.

Admittedly, the appropriate friction regime is in general difficult to identify from first principles, so claims of anomalous prefactors cannot be dismissed completely on the grounds of Kramer's theory. However, the suggested trend of rapidly decreasing diffusion prefactors with activation energy for weakly corrugated surfaces would be in conflict also with basic statistical mechanics. This can be understood in the following gedanken experiment: Consider an interface between two metals, *A* and *B*, at a surface, that may be crossed by a single adatom. The diffusivity as well as the binding energy of the adatom differ between the two subsystems in such a way that the transition state but not the binding sites are aligned in energy. The systems have an equal number of sites. The site-to-site jump rates, ν^A and ν^B, depend only on the barrier heights and the temperature. If the spatial probability distribution of the adatom is assumed to be stationary and in agreement with detailed balance—as required by microscopic reversibility—it can be shown that

$$\frac{P^{\mathrm{B}}}{P^{\mathrm{A}}} = \frac{\nu^{\mathrm{A}}}{\nu^{\mathrm{B}}}, \tag{7}$$

where P^{A} and P^{B} denote the probability of the adatom residing on surface A and B, respectively. On the other hand, the canonical distribution, evaluated within the harmonic approximation, yields

$$\frac{P^{\mathrm{B}}}{P^{\mathrm{A}}} = e^{-\Delta E_{\mathrm{AB}}/k_B T}\frac{\nu_0^{\mathrm{A}}}{\nu_0^{\mathrm{B}}}, \tag{8}$$

where the values of υ_0^{A} and ν_0^{B} are given by the fraction in Eq. (2) for the two surfaces, respectively. As a result,

$$\frac{\nu^{\mathrm{A}}}{\nu^{\mathrm{B}}} = \frac{\nu_0^{\mathrm{A}}}{\nu_0^{\mathrm{B}}} e^{-\Delta E_{\mathrm{AB}}/k_B T}. \tag{9}$$

Now, if surface A is "weakly corrugated" and surface B is not, the suggested anomaly in diffusion prefactors (which does not affect the exponentials) would be in conflict with Eq. (9), and thus violate a constraint imposed by basic statistical mechanics. Note that this argument does not in any way refer to the actual passage of a transition state; it therefore does not depend on the efficiency of equilibration, but only assumes that thermal equilibrium is eventually established.

To conclude this section, theoretical arguments appear to exclude the possibility of anomalous diffusion behavior at weakly corrugated surfaces. We now turn to critically assess the analysis methods of experimental data.

B. Island-density analysis

The anomalous prefactors reported in Ref. 7 have been determined from STM island-density analyses using the *nucleation-curve method* (NCM).[6,33] With this method, Arrhenius parameters for surface diffusion are determined by gathering island-density data using STM, and then analyzing these data within mean-field nucleation theory (MFNT).[17] The basic assumptions of MFNT are that (i) the density of isolated adatoms attains its mean value at every point on the terrace, i.e., the spatial dependence introduced by the presence of islands is neglected, and that (ii) the monomer diffusivity is constant. According to MFNT, the island density (the number of islands per surface unit cell), n_x, is under certain circumstances (see below) related to the monomer diffusivity, ν, through a *scaling law*:[17]

$$n_x = C\eta(\Theta, i)\left(\frac{F}{DN_0^2}\right)^{\chi} \exp\left(\frac{E_i}{(i+2)k_B T}\right). \tag{10}$$

Here i denotes the *critical* cluster size, i.e., the number of atoms in the smallest stable nucleus minus one, E_i its binding energy, $\chi = i/(i+2)$, $\eta(\Theta, i)$ a universal function of the coverage Θ, and C a geometry factor of order unity. If the smallest stable cluster at a given set of experimental conditions is the dimer, as is often the case, then $i=1$ and $E_i = 0$, so Eq. (10) simplifies to

$$n_x = C\eta(\Theta)\left(\frac{F}{DN_0^2}\right)^{1/3}. \tag{11}$$

Together with Eq. (1), this expression yields an Arrhenius relation for the temperature dependence of the island density n_x. For the experimental deduction of the two rate parameters, the values of C and η can be calculated in a fairly straightforward fashion,[17] and the parameters E_d and ν_0 then obtained from an analysis of the measured temperature dependence of n_x. Compared with more direct methods, the advantages of this method are that the measurements are not plagued by tip-sample interactions, and that they can be carried out over a wide temperature range. The disadvantage lies in the necessity to explicitly or implicitly make assumptions about microscopic processes involved in the nucleation and growth processes. In particular, the effects of small-cluster mobility[34] and instability[35] have been shown to com-

TABLE I. Comparison between *ab initio* and experimental values for the activation energies and preexponential factors of monomer diffusion for various metal systems. The experimental values are taken from Ref. 7, the theoretical values for Ag/Ag(111) and Ag/*s*-Ag(111) from Ref. 26. The *s* in *s*-Ag(111) denotes a strained system [1 ML of Ag on Pt(111)].

	Experiment [a]		Theory	
System	E_d (meV)	ν_0 (s^{-1})	E_d (meV)	ν_0 (s^{-1})
Ag/Ag(111)	97 ± 10	$2\times10^{11\pm0.5}$	82	8×10^{11}
Ag/*s*-Ag(111)	60 ± 10	$1\times10^{9\pm0.6}$	60	1×10^{12}
Al/Al(111)	42 ± 4	$8\times10^{6\pm0.25}$	42	4×10^{12}
Al/Au(111)	30 ± 5	2×10^{3}	120	7×10^{12}

[a]See Reference 63.

plicate the analysis considerably when present. For most systems, however, a temperature window can be identified where single-adatom diffusion is activated but clusters are immobile and stable with respect to dissociation.[33]

The NCM has been successfully applied to a wide range of epitaxial metal systems.[36] However, for certain systems with small activation energies to surface diffusion, this method has yielded extremely small diffusion prefactors, deviating up to ten orders of magnitude from expected values, and in disturbingly pronounced disagreement with theoretical state-of-the-art calculations (Table I). Barth and coworkers[7] have interpreted this anomaly to involve a novel regime of temperature-activated diffusion for weakly corrugated systems. The question is whether mean-field nucleation theory as expressed in Eq. (11) applies to those systems.

In the context of the NCM, an (apparent) low prefactor corresponds to a high island density. The inclusion of dimer mobility and instability, as well as long jumps (i.e., events where an atom crosses several saddle points without relaxation) in the analysis therefore cannot resolve the puzzle, as they all lead to lower island densities.[33]

The significance of small activation energies may lie in the relative sensitivity of the jump rate to small fluctuations in E_d. Possible sources of such fluctuations include interactions with step edges,[37,27,38] surfactants,[39] and adatoms of the same kind. The first two effects can be made arbitrarily small in an ideal experiment, but the latter is an inherent feature of nucleation. Adatom-adatom interactions are completely discarded in MFNT, and actually also in all previous models of homogeneous nucleation. It is then appropriate to ask how strong such interactions can be and if their character makes them prone to affect nucleation.

III. ADSORBATE INTERACTIONS

The strongest interaction between adsorbed atoms is the covalent chemical bond. Since this *direct* interaction originates in the energy gained from the overlap of atomic orbitals, its strength decays exponentially with the adatom-adatom separation d. This interaction thus dominates energetically only for the very shortest adsorbate separations, i.e., $d/a \lesssim 1$ (a being one surface-atomic lattice spacing). Similarly, adatoms can sense each other through direct Coulomb interactions between the various multipole moments that arise due to surface-induced charge redistribution on the adsorbates. These interactions decay asymptotically as $1/d^3$, and are typically relatively weak.[27]

Of potentially greater importance, then, are indirect interactions originating in the adsorbate-induced polarization of the surface-electron gas.[40–43] These interactions decay as $\cos(2q_F d)/d^5$ (Refs. 41 and 42) if mediated through bulk bands, and as $-\sin(2q_F d)/d^2$ (Refs. 41–43) in the presence of a semifilled surface band. In addition to these electronic interactions, an elastic interaction arises from adsorbate and substrate relaxations mediated via the atomic lattice,[44] which falls off as $1/d^3$ for asymptotically large separations.[45] A paramount problem with these asymptotic limits is that very little is known about the relative strength of all these interactions, and how large the adsorbate separations need to be for the power laws to be valid. As we will show below, the asymptotic laws are often not valid in the intermediate regime where most of the perturbation to the mean-field approach takes place. These contributions thus have to be gathered from full electronic structure calculations, or from correspondingly demanding experimental analyses.

A. Computational details

In this study, direct and indirect adatom-adatom interactions are quantified from first principles for three metal systems: Al/Al(111), Cu/Cu(111), and Al/Al(100). The calculations are based on density-functional theory (DFT),[46,47] using a pseudopotential method to describe core-valence interactions, as implemented in the highly efficient VASP (Ref. 48) and DACAPO (Ref. 49) codes. For the exchange-correlation functional, the local-density approximation (LDA) (Ref. 50) is used for Al(111), and the generalized gradient approximation (GGA) (Ref. 51) for Cu(111) and Al(100). The choice of exchange-correlation functional has previously been shown to affect only the quantitative details of the adsorbate interactions.[44] The one-electron wave functions are expanded in a plane-wave basis with an energy cutoff of 9.0, 17.2, and 11.0 Ry for Al(111), Cu(111), and Al(100),[52] respectively, using ultrasoft Vanderbilt pseudopotentials.[53] The Brillouin zone is sampled via the Methfessel-Paxton scheme.[48] The Kohn-Sham equations are solved self-consistently, and the atomic structure is optimized until residual forces on all unconstrained atoms are less than 0.03 eV/Å, which yields total-energy convergence down to the 1-meV level.

To reduce image interactions, the periodic supercells used in the calculations span at least twice the maximum adsorbate-adsorbate distance examined in a specific direction. Our supercells contain 14×4×6 (336) atoms in the case of Al(111), 12×4×4 (192) atoms for Cu(111) (computer memory constraints prohibit bigger cells for Cu), and 5×4×8 (160) atoms for Al(100). The smaller lateral cell size for Al(100) is motivated by the rapid convergence of the adsorbate interaction energy with increasing separation (see below). Above an additional surface layer containing the adsorbate atoms,[54] there is ≃9 (13) Å of vacuum for Al (Cu). The Brillouin zone is sampled using a 6×2, 3×1, 6×6 **k**-point mesh for Al(111), Cu(111), and Al(100), respectively. The dense sampling and large cells yield excellent energy convergence; atomic diffusion barriers and dimer binding energies for Al(111) on both unrelaxed and relaxed surfaces are within 2 meV of previous calculations using a 6×5×6 atom supercell and 6×6 **k**-point mesh.[44]

To separate electronic and elastic adsorbate interactions, all calculations are performed at two levels of relaxation. In one case, the slab (without adsorbates) is first fully relaxed, and the atomic coordinates then kept frozen in subsequent calculations. In the other case, all atoms are allowed to relax, save for the bottom two layers, which in both cases are fixed at bulk coordinates. In both instances, two atoms are adsorbed on top of the slab, and (always) allowed to fully relax. For Al/Al(111), one atom is placed in an hcp site (the preferred binding site at low coverage[37]), and the other atom is placed at consecutive hcp, bridge, and fcc sites along the ⟨110⟩ direction. In the Cu/Cu(111) calculations, one atom is placed in an fcc site, and the other in alternating bridge and fcc sites along the ⟨110⟩ direction. The maximum adatom-adatom separation is 17 (13) Å for Al (Cu), slightly less than half the length of the 41 (31) Å super cell so that image interactions should never exceed half the interaction energy at maximum separation. Saddle points for atomic diffusion are located by mapping out the total energy on a dense grid near bridge sites; in this case one or two of the lateral adsorbate coordinates are locked at each point on the mesh. The super cell geometries are illustrated in Figs. 1 [Al(111) and Cu(111)] and 2 [Al(100)].

B. Results

The computed adatom-adatom interaction energetics for Al/Al(111), Cu/Cu(111), and Al/Al(100) are displayed in Figs. 1 and 2. The adsorbate-adsorbate binding energy is defined with respect to two isolated adatoms, $E_{aa}=-E_2-E_0+2E_1$, where the subscript denotes the number of adatoms in the cell. The respective characteristics conform very well to the general magnitude of adsorbate interaction outlined above. In all three systems, the adsorbate-adsorbate binding energy is an order of magnitude larger for the shortest (dimer) bond than at larger separations [$E_{aa}|_{d=a}=0.52$, 0.26, and 0.26 eV for Al/Al(111), Cu/Cu(111), and Al/Al(100), respectively].

For Cu(111), the elastic energy is fairly constant within the range of adatom separations considered here, and the *variations* in E_{aa} (beyond the direct dimerization regime) are

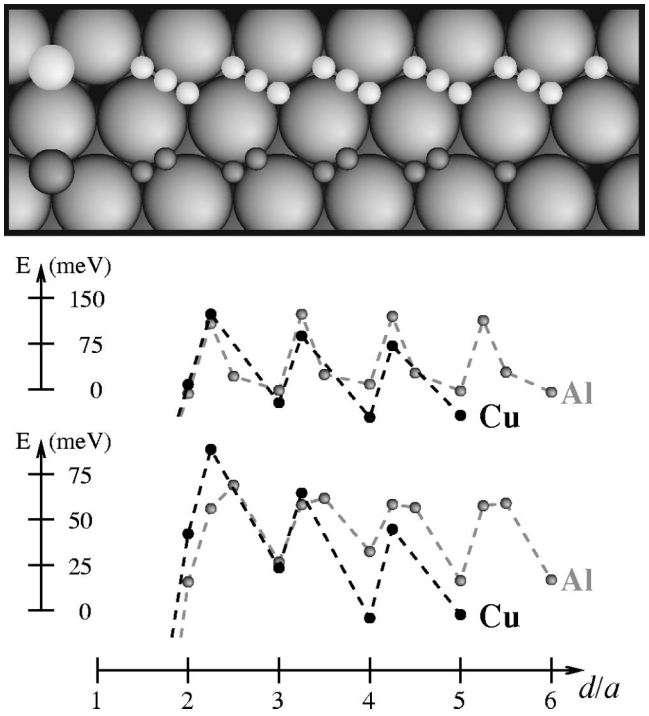

FIG. 1. Top view of adsorption geometries in the DFT calculations for Al/Al(111) and Cu/Cu(111). One adatom is placed at its preferred binding site (hcp for Al and fcc for Cu; midsize circles), and another atom is then placed at successive binding sites and saddle points (tiny circles) along the ⟨110⟩ direction (half the length of the Al supercell is shown). The energy is defined as $E=E_2+E_0-2E_1$, where the subscript denotes the number of adatoms in the cell, and is shown as a function of adsorbate separation d/a, a being a surface lattice parameter. Both frozen (middle graph) and relaxed (bottom graph) cases are truncated at short separations to enhance resolution.

mainly electronic. These long-range variations are attributed to the existence of a surface band, which has very convincingly been observed experimentally (STM) to result in the periodic ordering of sulphur[55] and copper[56] atoms on Cu(111). While we do note a long-range variation in the binding energy here as well, the supercell is too small to discern how well the periodicity agrees with the expected value of half the Fermi wavelength $\pi/q_F=15$ Å measured by Crommie *et al.*[57] In the case of Al(111), the electronic part of the interaction energy varies less, which is expected as the surface has no occupied surface-band states. However, the elastic energy is comparably large, and does not approach zero at the largest separations considered in this study.

In passing, we note that similar long-range interactions have also been noted recently for adsorption of nonmetals on close-packed metal surfaces,[58] where repulsive interactions between the fragments of dissociated O_2, NO, and N_2O species have been found to extend several lattice sites away. The strength of these indirect interactions increases along the series Pt(111), Au(111), Cu(111), corresponding to increasing surface-band occupancy.[58] Similar conclusions have recently been drawn in STM studies of oxygen diffusion on Ru(0001), where oxygen atom residence times have been

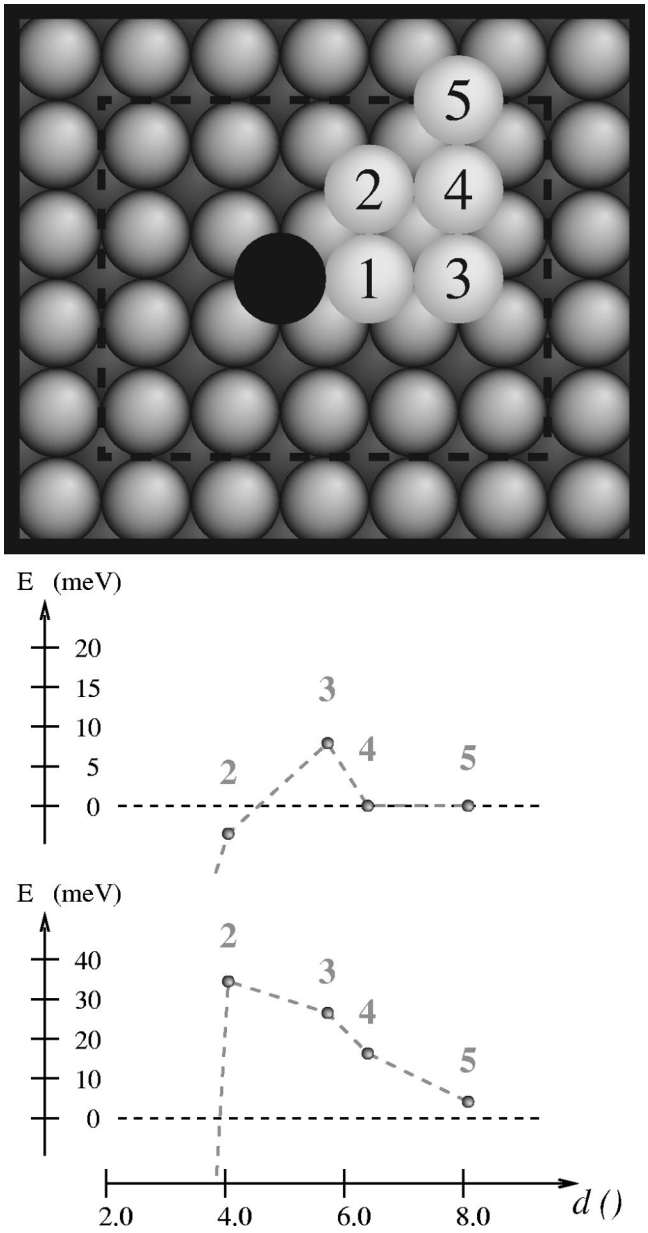

FIG. 2. Adsorption geometry for Al(100). One adatom is fixed (black), and the other one (yellow) is placed at sites 1–5. The dashed line in the top figure marks the size of the supercell. The binding energy is defined as in Fig. 1 and shown as of adsorbate separation d in angstroms for the cases of frozen (middle graph) and relaxed (bottom graph) substrates. Some of the values for the relaxed case have been reported previously (Ref. 63).

found to vary by more than an order of magnitude, depending on the local O coverage.[59]

For Al(100), the electronic part of the indirect interaction energy is very small (virtually zero beyond $d \simeq 2a$) and the adatom-adatom repulsion is predominantly elastic. In the next-nearest-neighbor configuration, some remaining (direct) chemical bond amounts to a slightly positive binding energy in the unrelaxed case,[60] whereas the relaxed surface exhibits repulsive interaction. The adsorbate interaction at the two largest separations in this study (6.4 and 8.1 Å, respectively) are exclusively elastic, as measured by computing adsorbate interactions while freezing lattice relaxations. The decrease in the elastic interaction energy between these two points (labeled ''4'' and ''5'' in Fig. 2) is much too large to be consistent with a $1/d^3$ falloff of the elastic energy. Consequently, the asymptotic limit,[45] which only accounts for surface relaxations and not adsorbate relaxations,[44] is reached at even larger distances, where almost all of the binding energy has already decayed. Hence, it is generally unreliable to separate electronic and elastic interactions by postulating a $1/d^3$ dependence for the latter, as attempted in Ref. 61.

We now turn to discuss how indirect adsorbate interactions affect adatom diffusion. The total-energy variations at binding sites and saddle points lead to variations in the atomic diffusion barrier in the proximity of another adatom. In the next-nearest-neighbor positions, the barriers to dimerization are so low that nucleation is spontaneous at even very low temperatures.[62,63] For that reason, the following discussion focuses on monomer diffusion at larger separations. We note first that for the close-packed surfaces, indirect interactions lead to fluctuations in the activation energy of 20–30 meV (Table II). When the elastic surface response is frozen out, this amounts to no more than a fourth of the ''unperturbed'' activation energy, which sets the relevant energy scale. Once substrate relaxations are allowed, the surface corrugation is smoothened out, so that the $|E_d^* - E_d|/E_d$ ratios—E_d^* (E_d) being the atomic diffusion barriers with (without) adsorbate interactions—are tripled and approach unity.

For the open Al(100) surface, the fluctuations in E_d (Ref. 64) are of the same magnitude as on the (111) surfaces, but the (relaxed) adatom diffusion barrier is more than an order of magnitude larger. Hence, the present study does not support the notion[7] that the strength of adatom interactions should scale with the amplitude of the surface corrugation. In fact, the same observations have also been made in first-principles calculations for a wide variety of chalcogen compounds on various metals.[58]

TABLE II. DFT values for the atomic diffusion barrier in the case of an isolated adatom (E_d) and the range of variation in barriers produced by the presence of another adatom (E_d^*) on the frozen and relaxed substrates. All values are in meV.

	Frozen		Relaxed	
System	E_d	E_d^*	E_d	E_d^*
Al/Al(111)	115	110–126	42	24–53
Cu/Cu(111)	134	110–146	50	41–69
Al/Al(100)	569		570	~540–570 [a]

[a]See Reference 63.

IV. GROWTH SIMULATIONS

In order to assess the effects of indirect adsorbate interactions on the surface morphology, we perform a set of kinetic Monte Carlo (KMC) (Ref. 30) simulations of the low-temperature growth of Al(111).

A. The KMC model

By describing elementary atomic processes in terms of discrete reaction events instead of explicitly calculating the trajectories, the KMC method renders the time and length scales of typical growth experiments accessible to materials theorists. In each algorithmic step, an atomic process is picked at random from a list of possible processes, so that the probability for each process is weighted by its TST rate. In contrast to equilibrium Monte Carlo methods, the KMC method is meant to reflect the actual time evolution of a system, and its predictive power has been demonstrated for a wide range of epitaxial systems.[6,66,67]

The activation energy for the diffusion of isolated Al atoms on Al(111) is 42 meV within DFT-LDA.[37,16] In the kinetic simulations, this value is subject to adjustments from interactions with nearby adatoms, as inferred from Fig. 1. In contrast to the simplified approach in Ref. 15, these modifications are all derived from DFT-computed variations at both binding sites *and* transition states, i.e., no empirical *a priori* presumptions are made about the energy variations at the saddle points. Possible angular dependencies of interaction energies are unknown, and therefore neglected, i.e., the energy shift of an adatom due to the presence of another adatom is assumed to be constant on regular hexagons centered on the latter. Interactions between more than two adatoms are assumed to be described by pairwise summation. Theoretical studies[41] and a recent STM study[61] suggest that this is a good approximation at a distance beyond the shortest adatom separations.

Ideally, the DFT results should extend to the adatom-adatom distances where all interactions have died out. In practice, though, some binding energy of the adatom pair remains even at the largest separations attainable in the large supercells used in this study. For Al/Al(111), the binding energy remainder is as large as 17 meV (repulsive), and has to be accounted for. As we surmise below, adatom-adatom repulsion affects the island density more, the more long range it is. We therefore choose a conservative setting for the cutoff separation, $d_{\mathrm{cutoff}}/a=6$, so that all of the remaining binding energy falls off to zero in going from $d/a=6$ (the largest separation in the DFT calculations) to $d/a=7$ lattice spacings (see Fig. 3).

For atomistic processes at kinks, corners, and edges of islands, we use exclusively first-principles-computed activation energies for Al/Al(111) reported in Ref. 65. However, at the relatively low temperatures considered here, these processes are so rare that they only marginally affect the island density.

In the simulations, atoms are deposited at random on an initially clean surface and allowed to diffuse on a close-packed lattice with periodic boundary conditions. The deposition flux, F, is 0.01 ML/s, and the coverage 5%. Convergence with respect to lattice dimensions is tested extensively using lattice areas of 200×200, 300×300, and sometimes 1200×1200 sites. Diffusion rates are assigned according to TST with DFT-computed activation energies (for exceptions, see below) and a common prefactor of 6×10^{12}Hz. As $n_x \propto \nu_0^{-\chi}$, with $\chi\lesssim\frac{1}{3}$ (as further discussed below), the choice of ν_0 will have only a minor effect on n_x, as long as it lies within the range of normal prefactor values.

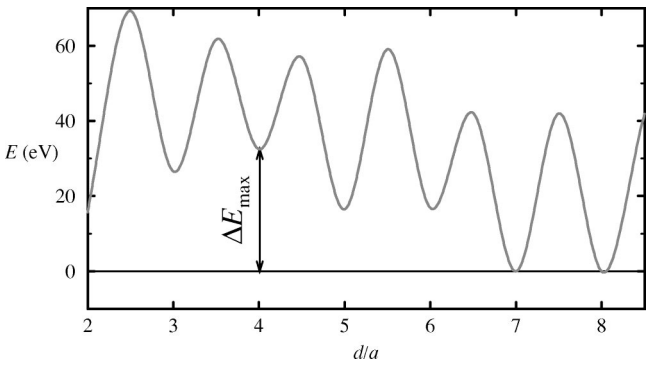

FIG. 3. Schematic of potential-energy landscape for an Al atom on the Al(111) surface at a distance of d/a lattice sites from another Al atom, as employed in the KMC simulations. Energies from two or more close adatoms are added pairwise.

B. Results

The results for the calculated Al/Al(111) island densities at $T=50$–75 K appear in Fig. 4 together with experimental data from Ref. 7. Without adatom interactions, the simulated island density exhibits normal scaling behavior, but it is consistently more than two orders of magnitude smaller than experimental values. With adsorbate interactions, however, n_x is enhanced tremendously, and the discrepancy between theory and experiment is virtually removed. However, as the

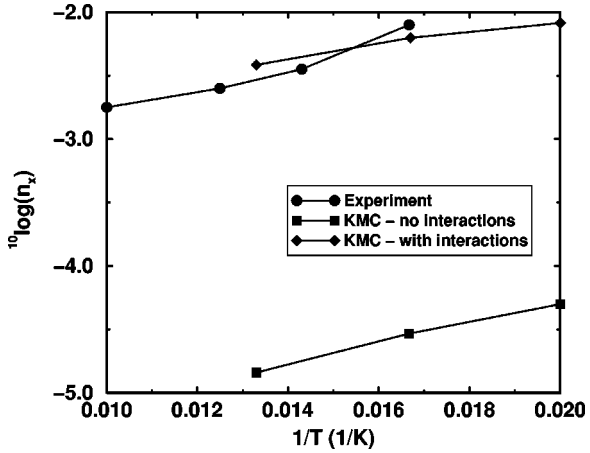

FIG. 4. Island density as a function of inverse temperature from STM experiments[7] and from KMC simulations performed with and without adatom interactions. To account for the somewhat lower coverage and higher growth rate in the simulations ($\Theta_{\mathrm{KMC}}/\Theta_{\mathrm{STM}}=5\%/15\%$, $F_{\mathrm{KMC}}/F_{\mathrm{STM}}=0.01/0.000\,64$), the experimental densities are shifted to $^{10}\log(n_x)+0.40$, as prescribed by nucleation theory.

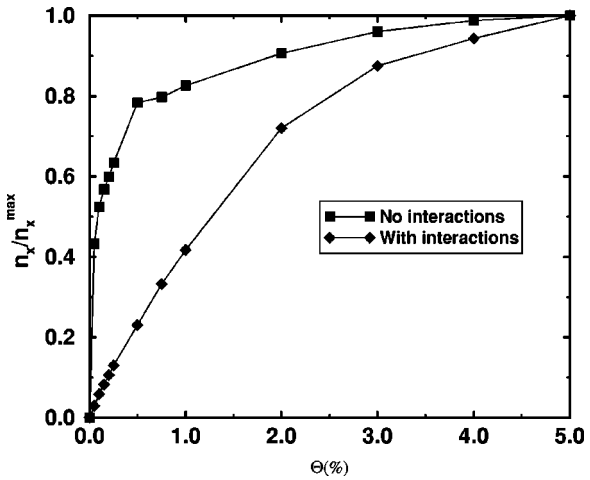

FIG. 5. Island density n_x as a function of coverage Θ from KMC simulations with adatom interactions present (diamonds) and absent (squares), both normalized to $n_x(\Theta=5\%)$.

accuracy of the island-density data presented in Ref. 7 has been questioned recently,[19] this agreement should not be considered to be proof of the quantitative predictive power of the theory. The decrease of n_x with increasing T is somewhat slower in the KMC simulations than in the experiments. If interpreted by means of MFNT, it would correspond to a computed apparent activation energy of ~ 30 meV, slightly less than the 42 meV measured in the experiment. However, the values are so close that the previously noted[7] similarity of E_d^{STM} to E_d^{LDA} for Al/Al(111) can hardly be brought forward as an argument against adsorbate interactions as the origin of alleged anomalous diffusion prefactors. The apparent prefactor, deduced from the same MFNT interpretation of the KMC-computed nucleation curve, would be 1×10^6 s^{-1}, i.e., close to the experimental value, 8×10^6 s^{-1}.[7]

The augmentation of the island density originates in the repulsive character of the adatom-adatom interactions. Assuming pairwise additive interactions, this repulsion hampers single adatoms from attaching to monomers and existing islands. Nucleation is thus postponed (see Fig. 5), and the monomer density increases markedly[68] (by more than an order of magnitude at 50 K), compared with the same simulation devoid of indirect interactions. Consequently, the probability of island nucleation via dimer formation instead of island growth via adatom attachment to an existing island is greatly enhanced. This is the origin of the greatly increased island density, when indirect interactions are correctly accounted for.

Fichthorn and Scheffler[15] have rationalized this augmentation of the island density by a simple empirical model, where the interaction is replaced by a uniform repulsive ring around each adatom. At the lowest temperatures, nucleation occurs only when adatoms happen to land within such a ring. The island density is then maximal and independent of T. As the temperature is raised, adatoms become increasingly more able to penetrate the rings to form nuclei in the earliest stages. However, the present system is far from the saturated low-temperature regime. When at 50 K deposition is prohibited within the "repulsive area," (where $E_{aa}<0$), the island density does not change. Instead n_x increases with the range of the repulsive interaction. If the repulsive area is decreased, so that $d_{\mathrm{cutoff}}=4$ with the maximum binding-energy difference, ΔE_{max} (as defined in Fig. 3), fixed, the island density at 50 K is decreased by a factor of ~ 40. Adatoms that have entered the repulsive area have higher chances of reaching another adatom to form a stable dimer bond before it leaves the area the *smaller* the area. Apparently, the entire range of possible behaviors in a system cannot be spanned by simply varying the strength of the repulsion, as assumed in Ref. 15. A detailed microscopic model thus has to include also the range of the interaction.

TABLE III. Scaling exponent, χ, for KMC-simulated growth of Al/Al(111) with adatom interactions present and absent, determined from the increase of n_x with deposition flux, F, in the range 0.01–0.1 ML/s. "Low prefactor" refers to the case where interactions are absent, but n_x is augmented by a very small monomer diffusion prefactor.

T (K)	50	60	75
With interactions	0.06	0.07	0.14
Without interactions	0.37	0.36	0.42
Low prefactor	0.19	0.28	0.32
Low prefactor, no dimer mobility	0.19	0.25	0.28

How can effects of interactions be distinguished from effects of anomalous prefactors, given a nucleation curve? In fact, the simulated island density at 50 K obtained with adsorbate interactions can be reproduced without interactions but with a prefactor ν_0 for monomer diffusion of $\sim 10^6$ s^{-1}, with the activation energy fixed. However, analyzing the $n_x(T)$ curve with this value of ν_0 with Eq. (11) yields a diffusion barrier of 62 meV. This deviates from the input value 42 meV for two reasons: (i) the high island density puts the system slightly outside the linear-scaling regime[33] and (ii) n_x is lowered by dimer diffusion [with a barrier of 130 meV (Ref. 62)], which is not accounted for in Eq. (11). If dimer diffusion is assumed to be frozen out, the deduced barrier is lowered to 35 meV, and low prefactors and adsorbate interactions would explain experimental results almost equally well.

In general, activation energies for monomer and dimer diffusion are not known prior to the analysis, so violations of the mean-field assumptions may be hard to detect this way. However, according to MFNT there is a wide range of island densities within which the scaling of n_x with F does not depend on any internal parameters.[33] The usual scaling law is $n_x \propto F^{\chi}$ with $\chi=\frac{1}{3}$, but at the quite high island densities considered here, the exponent is somewhat lower.[33] Table III shows that the scaling exponent is consistently and significantly smaller than that of an anomalous prefactor in the range $F=0.01$–0.1 ML/s^{-1} for the case of repulsive interactions. Indeed, values of χ significantly below the predictions of MFNT have been observed experimentally for the Al/Al(111) system.[69] We thus suggest that whether experimentally found high island densities originate in low prefac-

tors or repulsive adsorbate interactions can be settled by determining the scaling exponent.

As for the quantitative agreement with experiment, not much can be said at this point, due to the difference between the results presented in Refs. 7 and 19. Comparing with the latter, our KMC-simulated results for the island density is about an order of magnitude too large when accounting for adsorbate interactions and an order of magnitude too small when neglecting them. However, our ability to make quantitative predictions is limited by a number of approximations, as outlined above, and even if the results of Michely *et al.* turn out to be closer to those of a perfect experiment, that would not overthrow our main conclusions.

Finally, it should be pointed out that all anomalous prefactors in surface diffusion cited here[7–10,13] (Ref. 12 being an exception[18]) have been obtained with indirect methods and analyses that require adsorbate interactions to be small.

V. CONCLUSIONS

Extensive DFT calculations of short- and long-range adsorbate interactions at both binding sites and transition states are used to study the effect of adsorbate interactions on the epitaxial growth of Al(111) by means of kinetic Monte Carlo simulations. When the DFT-computed adsorbate interactions are invoked into the KMC calculations, the simulated island density is in good agreement with experimental data. If long-range interactions are neglected, i.e., the atomic diffusion barrier is assumed to be unaffected by neighboring adatoms beyond the dimerization regime, the simulated island density is found to decrease by more than two orders of magnitude. Since experimental analyses within the mean-field framework neglect to account for adatom interactions, whereas the island density they measure inherently include such contributions, too-low prefactor values are systematically deduced for systems, where interactions raise the island density. In the particular case of Al/Al(111), a mimicking of the experimental MFNT analysis of the correct island-density data (including adsorbate interactions) gives a prefactor that is artificially lowered by more than six orders of magnitude. Of course, there is no question that this deduction process yields an incorrect value, as the prefactor is an input parameter in the KMC simulations (preset at $\nu_0 = 6 \times 10^{12}$ s^{-1}).

To summarize, an oversimplified analysis of island-density data can result in such anomalous values of the diffusion prefactors that have been reported in STM growth studies. By correctly accounting for medium- and long-range adsorbate interactions in a weakly corrugated adsorbate system, we show that the prefactor anomaly is lifted to yield a value in good agreement with direct theoretical calculations and the expected universal prefactor value of about 1–10 THz. We show that interactions modify the scaling of the island density with deposition flux, which could be used as an experimental signature of adsorbate interactions. The magnitude of the indirect interactions do not generally scale with the adatom diffusion barrier, which explains why the allegedly anomalous prefactors have been observed exclusively in systems with a weak surface corrugation. We also review the present theoretical view of adsorbate diffusion on metallic substrates, and show that extremely small diffusion prefactors actually are inconsistent with basic diffusion theory and statistical mechanics. A theoretical framework is developed to deal with weakly corrugated adsorbate systems.

In our view, whenever anomalous diffusion behavior is observed in the classical regime, alternative interpretations of experimental data should be sought. Specifically, the nucleation-curve method could be complemented with a more direct method for observing surface diffusion when both activation energies and prefactors come out very small. As an important corollary, once we accept that these prefactor anomalies are misconstrued, and that to date we know of no convincing evidence that highly anomalous prefactors exist in condensed-matter systems, then we also need to be very critical of kinetic models whose functionality relies on use of nonstandard prefactors.

ACKNOWLEDGMENTS

We would like to acknowledge stimulating discussions with Harald Brune. This work was partially supported by the Swedish Research Council for Engineering Sciences (TFR) and the Foundation for Strategic Research (SSF). Allocation of computer time at the UNICC facilities at Chalmers University of Technology is gratefully acknowledged.

APPENDIX AL/AU(111)

In this appendix, the theoretical determination of the Arrhenius parameters for the Al/Au(111) system appearing in Table I is presented, and the interpretation of experimental data is briefly discussed.

The atomic diffusion of Al atoms on Au(111) has been studied experimentally by Fischer *et al.*[70,9] A nucleation-curve analysis of the STM-measured island-density data yields an activation energy $E_d = 30$ meV, and a preexponential factor $\nu_0 = 2 \times 10^3$ s^{-1}. The prefactor value is highly anomalous in that it is extremely small (at ten orders of magnitude below what is considered normal, it is to our best knowledge the smallest prefactor ever reported in a surface diffusion study[7]) and thus at great variance with the present view of surface diffusion outlined in this paper. Here we show that the measured values of both E_d and ν_0 disagree severely with our first-principles calculations.

We use DFT within the GGA, applying a pseudopotential method and a plane-wave basis set with a cutoff energy of 25 Ry. The supercell contains a slab of five (2×2) atomic layers, one adatom, and a 12-Å vacuum region. The surface Brillouin zone is sampled with a dense 8×8 **k**-point mesh. For convergence tests and dimer calculations a (3×3) slab with a 5×5 **k**-point mesh is used, as indicated below. The bottom two atomic layers are kept at bulk positions, while the remaining layers are allowed to relax until the residual forces on all unconstrained atoms are less than 0.03 eV/Å.

Experimentally, the Au(111) surface is found to exhibit a long-range stacking-fault-domain structure with alternating regions of fcc and hcp termination and a $\begin{pmatrix} 22 & 0 \\ -1 & 2 \end{pmatrix}$ surface unit cell.[71,72] In our calculations, all barriers and binding energies are computed for both fcc and hcp termination, and thus both

TABLE IV. Total energies in meV for the Al/Au(111) system. The stacking is labeled "ABCAB" and "ABCAC" for fcc and hcp termination, respectively.

Top layer	A	B	C	Bridge
fcc	26		0	129
hcp	23	0		127

environments experienced by the diffusing Al atoms are surveyed, save for the actual stacking-fault boundaries.

The calculated activation energies and binding energies are summarized in Table IV. The most unexpected result is that the computed value for the atomic diffusion barrier, 0.13 eV for both fcc and hcp termination, is more than four times larger than the value reported in Ref. 9. For a $3\times3\times5$ unit cell the barrier is 0.12 eV, implying excellent convergence. The DFT-computed prefactor for this process (fcc termination) is 7×10^{12} s^{-1} [calculated using Eq. (2) with $N=1$], i.e., quite normal and over nine orders of magnitude larger than the experimental value reported in Ref. 9.

In accordance with experiments,[70,9] we find surface-atom exchange with the substrate to be energetically favorable with an energy gain of 0.67 eV. The Au atom ending up in the adsorbate layer is bound to the Al atom in the surface layer with a binding energy of about 0.4 eV, which confirms the experimental observation that single Au atoms are immobile and serve as nucleation sites.

The assumption of dimer stability below 230 K (Ref. 9) is not corroborated in the present study; the binding energy at the fcc-terminated surface is only 0.05 eV, implying an activation temperature for dimer dissociation of less than 100 K.

The medium-range adatom-adatom repulsion discussed in the main text exists for this system also: at two surface lattice sites separation, the binding energy of the Al dimer on the fcc-terminated Au(111) surface is -0.10 eV, which is of the same magnitude as the monomer diffusion barrier. Considering the substantial disagreement between the experimentally deduced and DFT-calculated values of activation energy and prefactor for monomer diffusion and the dramatic effect of adatom-adatom interaction on the island density, we conclude that adsorbate interactions are likely to lie behind extremely high island densities in this system as well.

[1] H. Eyring, J. Chem. Phys. **3**, 107 (1935); S. Glasstone, K. J. Laidler, and H. Eyring, *The Theory of Rate Processes* (McGraw-Hill, New York, 1941).

[2] P. Hänggi, P. Talkner, and M. Borkovec, Rev. Mod. Phys. **62**, 251 (1990).

[3] G. Wahnström, in *Interaction of Molecules with Solid Surfaces*, edited by V. Bortaloni, N. M. March, and M. P. Tosi (Plenum Press, New York, 1990).

[4] V. P. Zhdanov, Surf. Sci. Rep. **12**, 183 (1991).

[5] R. Gomer, Rep. Prog. Phys. **53**, 917 (1990).

[6] H. Brune, Surf. Sci. Rep. **31**, 121 (1998).

[7] J. V. Barth, H. Brune, B. Fischer, J. Weckesser, and K. Kern, Phys. Rev. Lett. **84**, 1732 (2000).

[8] H. Brune, K. Bromann, H. Röder, K. Kern, J. Jacobsen, P. Stoltze, K. Jacobsen, and J. Nørskov, Phys. Rev. B **52**, 14 380 (1995).

[9] B. Fischer, H. Brune, J. V. Barth, A. Fricke, and K. Kern, Phys. Rev. Lett. **82**, 1732 (1999).

[10] J.-R. Chen and R. Gomer, Surf. Sci. **94**, 456 (1980).

[11] J. R. Banavar, M. H. Cohen, and R. Gomer, Surf. Sci. **107**, 113 (1981).

[12] B. G. Briner, M. Doering, H.-P. Rust, and M. Bradshaw, Science **278**, 257 (1997).

[13] E. Nabighian and X. D. Zhu, Chem. Phys. Lett. **316**, 177 (2000).

[14] G. L. Kellogg, Surf. Sci. Ref. **21**, 1 (1994).

[15] K. A. Fichthorn and M. Scheffler, Phys. Rev. Lett. **84**, 5371 (2000).

[16] A. Bogicevic, S. Ovesson, P. Hyldgaard, B. I. Lundqvist, H. Brune, and D. R. Jennison, Phys. Rev. Lett. **85**, 1910 (2000).

[17] J. A. Venables, G. D. T. Spiller, and M. Hanbücken, Rep. Prog. Phys. **47**, 399 (1984); J. A. Venables, Phys. Rev. B **36**, 4153 (1987).

[18] In Ref. 12, the diffusion of CO on Cu(110) is monitored directly with the STM and found to have a preexponential factor of 3×10^{7} s^{-1}. It is not clear, however, whether the diffusion of CO on Cu(110) is a simple one-step, one-channel process or a more complex motion.

[19] T. Michely, W. Langenkamp, H. Hansen, and C. Busse, Phys. Rev. Lett. **86**, 2695 (2001).

[20] G. H. Vineyard, J. Phys. Chem. Solids **3**, 121 (1957).

[21] Quantum corrections to this formula can be invoked [see P. G. Wolynes, Phys. Rev. Lett. **47**, 968 (1981) and E. Pollak, Chem. Phys. Lett. **127**, 178 (1986)], but with the exception of hydrogen, those corrections are always quite small.

[22] U. Kürpick, A. Kara, and T. S. Rahman, Phys. Rev. Lett. **78**, 1086 (1997); U. Kürpick and T. S. Rahman, Phys. Rev. B **57**, 2482 (1998).

[23] W. Meyer and H. Neldel, Z. Tech. Phys. (Leipzig) **12**, 588 (1937).

[24] G. Boisvert and L. J. Lewis, Phys. Rev. B **54**, 2880 (1996).

[25] A. F. Voter and J. D. Doll, J. Chem. Phys. **80**, 5832 (1984).

[26] C. Ratsch and M. Scheffler, Phys. Rev. B **58**, 13 163 (1998).

[27] R. Stumpf and M. Scheffler, Phys. Rev. B **53**, 4958 (1996).

[28] D. C. Senft and G. Ehrlich, Phys. Rev. Lett. **74**, 294 (1994).

[29] J. Jacobsen, K. W. Jacobsen, and J. P. Sethna, Phys. Rev. Lett. **79**, 2843 (1997).

[30] A. F. Voter, Phys. Rev. B **34**, 6819 (1986).

[31] Molecular-dynamics simulations of adatom diffusion for systems with low activation energies are reported in G. C. Kallinteris, G. A. Evangelakis, and N. I. Papanicolaou, Surf. Sci. **369**, 185 (1996), but that study does not discuss the accuracy of TST.

[32] H. A. Kramers, Physica (Amsterdam) **7**, 284 (1940).

[33] H. Brune, G. S. Bales, J. Jacobsen, C. Boragno, and K. Kern, Phys. Rev. B **60**, 5991 (1999).

[34] S. Liu, L. Bönig, and H. Metiu, Phys. Rev. B **52**, 2907 (1995).

[35] M. C. Bartelt, S. Günther, E. Kopatzki, R. J. Behm, and J. W. Evans, Phys. Rev. B **53**, 4099 (1996).

[36] See Table 2 in Ref. 6.

[37] R. Stumpf and M. Scheffler, Phys. Rev. Lett. **72**, 254 (1994).
[38] S. C. Wang and G. Ehrlich, Phys. Rev. Lett. **70**, 41 (1993); F. Watanabe and G. Ehrlich, J. Phys. Chem. **95**, 6075 (1991); **96**, 3191 (1992).
[39] S. Horch, H. T. Lorensen, S. Helveg, E. Lægsgaard, I. Steensgaard, K. W. Jacobsen, J. K. Nørskov, and F. Besenbacher, Nature (London) **398**, 134 (1999).
[40] T. B. Grimley, Proc. Phys. Soc. London **90**, 751 (1967); **92**, 776 (1967).
[41] T. L. Einstein and J. R. Schrieffer, Phys. Rev. B **7**, 3629 (1973); T. L. Einstein, Surf. Sci. Lett. **75**, 161 (1978); *Handbook of Surface Science*, edited by W. N. Unertl (Elsevier, Amsterdam, 1996), Vol. 1, p. 577.
[42] K. H. Lau and W. Kohn, Surf. Sci. **75**, 69 (1978).
[43] P. Hyldgaard and M. Persson, J. Phys.: Condens. Matter **12**, L13 (2000).
[44] A. Bogicevic, Phys. Rev. Lett. **82**, 5301 (1999).
[45] K. H. Lau and W. Kohn, Surf. Sci. **65**, 607 (1977).
[46] P. Hohenberg and W. Kohn, Phys. Rev. **136**, B864 (1964).
[47] W. Kohn and L. J. Sham, Phys. Rev. **140**, A1133 (1965).
[48] G. Kresse and J. Hafner, Phys. Rev. B **47**, 558 (1993); **49**, 14 251 (1994); **54**, 11 169 (1996).
[49] B. Hammer and L. Bengtsson, computer code DACAPO-1.30, (Denmark Technical University, Lyngby, Denmark, 1999).
[50] J. P. Perdew and A. Zunger, Phys. Rev. B **23**, 5048 (1981).
[51] J. P. Perdew *et al.*, Phys. Rev. B **46**, 6671 (1992).
[52] The different energy cutoffs for Al(111) and Al(100) merely reflect the use of different pseudopotentials.
[53] D. Vanderbilt, Phys. Rev. B **32**, 8412 (1985).
[54] The artificial electric field induced by one-sided adsorption is very weak; when compensated by a dipole layer in the vacuum, energy differences change by ≤ 10 meV, and (more importantly), by the same energy amount for different adsorption sites.
[55] E. Wahlström, I. Ekvall, H. Olin, and L. Wallden, Appl. Phys. A: Mater. Sci. Process. **A66**, S1107 (1998).
[56] J. Repp, F. Moresco, G. Meyer, K. Rieder, P. Hyldgaard, and M. Persson, Phys. Rev. Lett. **85**, 2981 (2000).
[57] M. F. Crommie, C. P. Lutz, and D. M. Eigler, Nature (London) **363**, 524 (1993).
[58] A. Bogicevic and K. C. Hass (unpublished).
[59] S. Renisch, R. Schuster, J. Wintterlin, and G. Ertl, Phys. Rev. Lett. **82**, 3839 (1999).
[60] The calculations for Al/Al(100) have been repeated without adsorbate relaxation in order to confirm the division of the total energy into electronic and elastic contributions, as described in the text. A single adatom is placed on the frozen substrate and allowed to relax. The calculations depicted in Fig. 2 are then carried out with both adatoms fixed in the positions that correspond to the one attained by the isolated adatom. Imposing these constraints, however, does not change the qualitative features of the binding curve in comparison with the case of frozen substrate with adsorbate relaxation.
[61] L. Österlund, M. Ø. Pedersen, I. Stensgaard, E. Lægsgaard, and F. Besenbacher, Phys. Rev. Lett. **83**, 4812 (1999).
[62] A. Bogicevic, P. Hyldgaard, G. Wahnström, and B. I. Lundqvist, Phys. Rev. Lett. **81**, 172 (1998).
[63] A. Bogicevic, S. Ovesson, B. I. Lundqvist, and D. R. Jennison, Phys. Rev. B **61**, 2456 (2000).
[64] E_d refers to a hopping diffusion process, i.e., diffusion via exchange with the substrate is not considered.
[65] A. Bogicevic, J. Strömquist, and B. I. Lundqvist, Phys. Rev. Lett. **81**, 637 (1998).
[66] P. Ruggerone, C. Ratsch, and M. Scheffler, in *Growth and Properties of Ultrathin Epitaxial Layers*, edited by D. A. King and D. P. Woodruff (Elsevier Science, Amsterdam, 1997).
[67] S. Ovesson, A. Bogicevic, and B. I. Lundqvist, Phys. Rev. Lett. **83**, 2608 (1999).
[68] For this reason the KMC simulations with interactions become very expensive: a single run with a 300×300 lattice can involve up to 3×10^{10} atomic jumps, which is more than 100 times more than without interactions.
[69] H. Brune (private communication).
[70] B. Fischer, J. V. Barth, A. Fricke, L. Nedermann, and K. Kern, Surf. Sci. **389**, 366 (1997).
[71] J. V. Barth, H. Brune, G. Ertl, and R. J. Behm, Phys. Rev. B **42**, 9307 (1990).
[72] A. R. Sandy, S. G. J. Mochrie, D. M. Zehner, K. G. Huang, and D. Gibbs, Phys. Rev. B **43**, 4667 (1991).